Anion effects on the redox kinetics of positive electrolyte of the all-vanadium redox flow battery

Matthäa Holland-Cunz, Jochen Friedl, Ulrich Stimming

PII: S1572-6657(17)30770-1
DOI: doi:10.1016/j.jelechem.2017.10.061
Reference: JEAC 3621

To appear in: *Journal of Electroanalytical Chemistry*

Received date: 12 August 2017
Revised date: 25 October 2017
Accepted date: 26 October 2017

Please cite this article as: Matthäa Holland-Cunz, Jochen Friedl, Ulrich Stimming , Anion effects on the redox kinetics of positive electrolyte of the all-vanadium redox flow battery. The address for the corresponding author was captured as affiliation for all authors. Please check if appropriate. Jeac(2017), doi:10.1016/j.jelechem.2017.10.061

Anion effects on the redox kinetics of positive electrolyte of the all-vanadium redox flow battery

Matthäa Holland-Cunz, Jochen Friedl, Ulrich Stimming*

School of Chemistry, Newcastle University Newcastle upon Tyne, NE1 7RU, UK.

*** Corresponding author: Prof. Stimming, Ulrich.Stimming@newcastle.ac.uk**

Keywords: Catalysis, Vanadium, Redox Flow Battery, Kinetics, Reaction Mechanism.

ABSTRACT

The VO^{2+}/VO_2^+ redox reaction takes place in the catholyte solution of the all-vanadium redox flow battery (VRFB), one of the few options to electrochemically store energy from intermittent renewable sources on a large scale. However, the sluggish redox kinetics of the VO^{2+}/VO_2^+ couple limit the power density of the VRFB, which increases the footprint of the power converters and increases capital costs. Therefore, catalysis of the redox reaction and a deeper understanding of its intricate reaction pathways is desirable.
The kinetics of the VO^{2+}/VO_2^+ redox reaction have been investigated in 1M sulfuric and 1 M phosphoric acid by cyclic voltammetry, chronoamperometry, electrochemical impedance spectroscopy and flow battery tests. It was found that in 1 M phosphoric acid the electron transfer constant k_0 is up to 67 times higher than in 1 M sulfuric acid. At higher over-potentials the determined currents match for the two electrolytes. This over-potential dependent difference in electron transfer constant is explained by variable contributions from three reaction mechanisms for the oxidation of VO^{2+} to VO_2^+, and by the presence of adsorbed intermediates for the reduction of VO_2^+. This study shows that the redox kinetics of the VO^{2+}/VO_2^+ can be considerably accelerated by altering the chemical environment of the vanadium ions, and that this effect can also be transferred into a flow battery.

1. INTRODUCTION

The all vanadium redox flow battery (VRFB) has become increasingly important as energy storage for renewable energies due to progressive global warming in recent years. The energy storage is based on the conversion of electrical into chemical energy in the form of soluble redox pairs. Compared to other energy storage systems, the VRFB offers essential

advantages: VRFB has a low self-discharge, long lifetime and high cycle stability [1,2]. Another advantage is that power and capacity can be scaled independently. Even with regard to safety aspects, the VRFB does not pose any major risks, as its components are not flammable and less toxic than other elements employed for redox flow batteries (RFBs). In contrast to iron / chromium or zinc / bromine RFBs, the advantage of the VRFB is that by using purely vanadium ions in catholyte and anolyte, no cross-contamination of both circuits occurs by diffusion of vanadium ions through the membrane which would cause irreversible loss of capacity. One of the remaining problematic challenges is the low power density (< 0.1 W/cm^2) due to slow kinetics of the VO^{2+}/VO_2^+ redox reaction. The electron transfer constant k_0 of aforementioned redox reaction is 1 - 3 10^{-6} cm s^{-1} on carbon electrodes [3] which indicates that the power density is limited by the charge transfer resistance. In addition, it was shown by Gattrell *et al.* that the redox reaction is not a simple electron transfer, but indeed a combination of two chemical (de-/protonation) reactions and an electron transfer [4,5]. The sequence of these steps is not fixed but their contribution depends on the applied over-potential and other parameters. To complicate things further, a deposition of vanadium oxides on carbon electrodes from the electrolyte has been observed [4,6,7]. To increase the power density of the VRFB catalysis of the vanadium reactions is desirable. However, we have shown that in contrast to the V^{2+}/V^{3+} redox reaction, the VO^{2+}/VO_2^+ couple is not catalyzed by oxygen functional groups on carbon electrodes [3,6,8,9]. Therefore, we are now investigating homogeneous catalysis by replacing the commonly employed sulfate ions by phosphate ions. In this study we show that transferring the system from 1 M sulfuric acid to 1 M phosphoric acid the electron transfer constant k_0 is increased. This observation is confirmed by chronoamperometry (CA), electrochemical impedance spectroscopy (EIS) as well as qualitatively by cyclic voltammetry (CV) and symmetric flow cell tests.

2. EXPERIMENTAL

Electrolyte: To prepare a solution of 50 mM VO^{2+} and 50 mM VO_2^+, 25 mM vanadium pentoxide and 50 mM vanadyl sulfate were added to the supporting electrolyte (1 M sulfuric acid, 1 M phosphoric acid, 0.5 M sulfuric acid / 0.5 M phosphoric acid) and heated to reflux until completely dissolved. After cooling to room temperature (RT) the solutions were used.

NMR: NMR spectra were recorded at room temperature with Bruker Avance III at a frequency of 300 MHz.

Electrochemical measurements: CVs, EIS and CA were conducted with a Bio-Logic SP-300 in a custom-built glass cell at RT. The used cell comprised a three-electrode set-up (mercurous sulphate reference electrode (MSE in 1 M sulfuric acid, 0.674 V vs. Standard hydrogen electrode (SHE)), gold counter electrode, glassy carbon working electrode (surface area A = 0.02 cm^2). For CV, CA and EIS experiments the geometric surface area was used to calculate the current density j from the current I. The concentration of the solutions were 50 mM VO^{2+} and 50 mM VO_2^+ in various electrolytes for CV, CA and EIS. Before each experiment nitrogen was passed through the solution and the working electrode was polished with 0.05 µm polishing alumina. Between each potential step the working electrode was polished again. The over-potential was applied in 50 mV steps in the range from ± 50 to ± 1000 mV. For the data analysis, the transients were fitted in the time regime from 0.25 to 0.40 $s^{1/2}$ in a current versus square-root of time plot. To conduct EIS the open circuit potential (OCP) was perturbed with a 10 mV amplitude in a frequency range from 40 kHz to 100 mHz. The data were fitted with EC-Lab. Cyclic voltammetry was carried out with a scan rate of 100 mV s^{-1}.

RFB cell tests: For flow cell tests a C Flow LAB 5x5 cell was used in conjunction with a Reglo ICC pump. GFD graphite felts (50 x 50 x 4.6 mm^3) from SGL Carbon were used as electrodes. The half-cells were separated by a Nafion N117 membrane. Before each battery test, the electrodes were heat-treated at 400°C for 12 h in laboratory atmosphere and the membrane was boiled in 1 M sulfuric acid for 30 min. Initially, both electrolyte tanks contained the same electrolyte, 50 mM VO^{2+} and 50 mM VO_2^+ in 1 M sulfuric or 1 M phosphoric acid, respectively, so that only the catholyte of a VRB was investigated. The experiments were conducted within an acrylic box at RT and both electrolyte tanks contained 60 ml of electrolyte and were continuously purged with nitrogen. The battery was charged and discharged by the potentiostat Bio-Logic SP-300 with currents from 25 to 2000 mA. The cut off potentials were ±1.0 V.

3. RESULTS

3.1 NMR

^{51}V NMR spectra were recorded to investigate the effect of the anion of the supporting electrolyte on chemical environment of the VO_2^+ ion. Vanadium is diamagnetic and susceptible for NMR in the oxidation states (-III, d^8), (-I, d^6) and (+V, d^0). Vanadium (+IV) is paramagnetic under normal conditions and cannot be observed [10]. As shown in Fig. 1, the

peak of VO_2^+ ion in 1 M sulfuric acid appears at -543.81 ppm and in 1 M phosphoric acid the peak is located at -556.81 ppm. When vanadium pentoxide is dissolved in a mixture of both supporting electrolytes, 0.5 M each, the peak appears between both peaks, at -550.56 ppm. This result indicates, that the coordinating environment of the VO_2^+ ion changes with the supporting electrolyte and the containing anions.

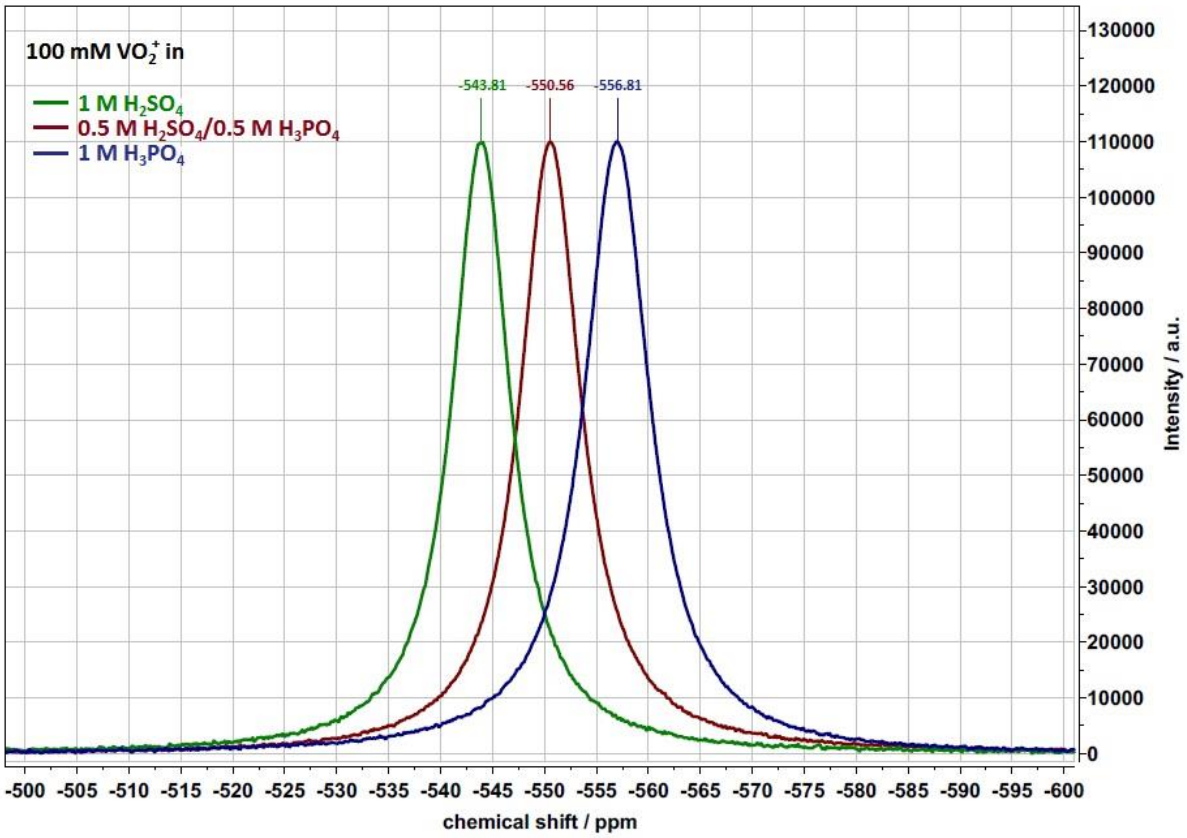

Figure 1 ^{51}V NMR spectra of 50 V_2O_5 dissolved in three different supporting electrolytes.

Around *pH* 1 vanadium (V) is present as the vanadyl cation VO_2^+ which has a cis-dioxo structure and the formation of the pseudo-octahedral species $[VO_2(H_2O)_4]^+$ is assumed [11]. In sulfuric acid and phosphoric acid the formation of sulfate/phosphate-compounds that still contain the octahedral cis-VO_2 is suggested. Gresser *et al*. showed that phosphate anions form anhydrides with vanadate and heteropolyvanadate ions can be formed [12]. The difference in chemical shift observed for the three supporting electrolytes suggests that both sulfate and phosphate anion interact with the VO_2^+ ion and that the result is a different vanadium-anion compounds in each solvent. The chemical shift is very sensitive to the chemical environment. We assume that in the mixed electrolyte the VO_2^+ ion undergoes a rapid anion exchange and appears as a single peak at the average chemical shift. This

phenomenon occurs when ions or molecules transform quickly between two states and the total magnetization, which does not dephase notably, emerges from all ions [13].

3.2 Cyclic Voltammetry

Figure 2 shows CVs of 50 mM VO^{2+} and 50 mM VO_2^+ in 1 M sulfuric acid (red), 1 M phosphoric acid (black) and in 0.5 M sulfuric acid / 0.5 M phosphoric acid (green). Apparent characteristic standard potentials calculated from the mean of anodic and cathodic peak potential are similar in all electrolytes, but differ greatly from the tabulated standard potential of U^{Θ} = 1.00 V vs. SHE [14] (see table 1). This might be due to the assymetry in the electron transfer reactions.

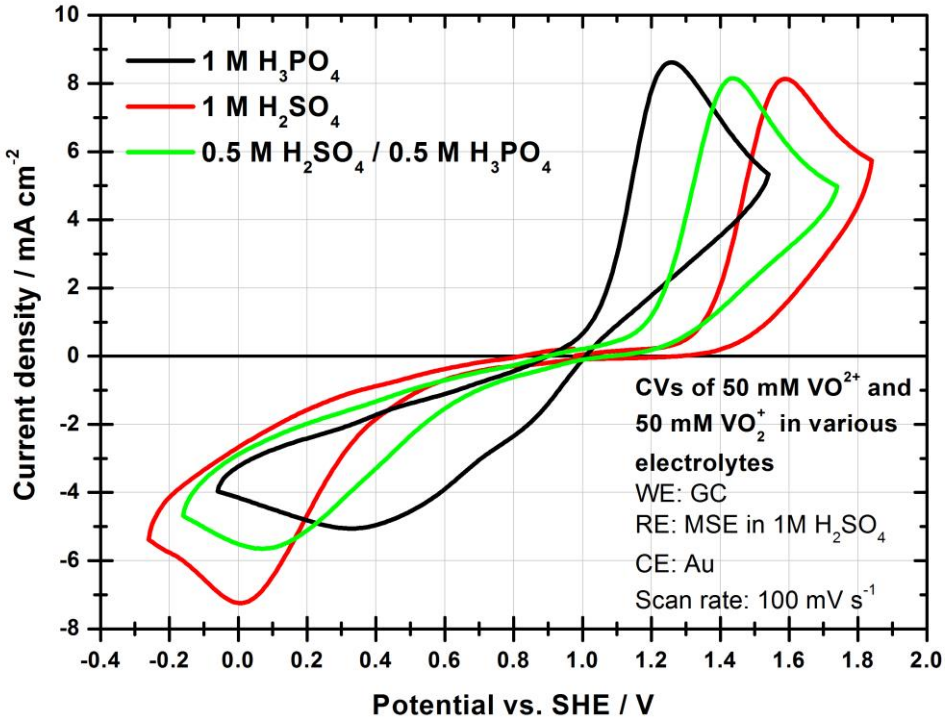

Figure 2 CVs of 50 mM VO^{2+} and 50 mM VO_2^+ in variuous electrolytes at a scan rate of 100 mV s^{-1}.

The anodic and cathodic peak potentials vary with electrolyte as shown in Table 1. The smallest peak separation can be found in 1 M phosphoric acid and the largest in 1 M sulfuric acid. The mixed electrolyte shows an intermediate separation. This may indicate that the kinetics of the redox reaction are faster in 1 M phosphoric acid than in the other electrolytes

because on flat electrodes a smaller peak separation suggests a higher electron trasnfer constant [3,15].

Electrolyte	apparent U^{Θ} / V vs. SHE	U_{peak}^{ox}/ V vs. SHE	U_{peak}^{red}/ V vs. SHE	Peak separation / V
1 M H_2SO_4	0.824	1.590	0.058	1.532
1 M H_3PO_4	0.793	1.257	0.328	0.929
0.5 M H_2SO_4 / 0.5 M H_3PO_4	0.752	1.437	0.067	1.370

Table 1 Parameters extracted from CVs of 50 mM VO^{2+} and 50 mM VO_2^+ in various electrolytes.

3.3 Electrochemical impedance spectroscopy

EIS was recorded for all three electrolytes and Nyquist plots and one representative Bode plot are shown in Fig. 3. By fitting the experimental spectra to the Randles circuit the parameters listed in Table 2 are obtained. The double layer capacitance C_{DL} is calculated from the constant phase element Q by the formula given by Hirschhorn *et al.* for a surface distribution [16]:

$$C_{\mathrm{DL}} = Q^{1/\alpha}\left(R_{\mathrm{Ohm}} \cdot R_{\mathrm{CT}} / R_{\mathrm{Ohm}} + R_{\mathrm{CT}}\right)^{(1-a)/a} \quad (1)$$

With ohmic resistance R_{Ohm}, charge transfer resistance R_{CT} and constant phase element parameter α. The electron transfer constant k_0 is given by:

$$k_0 = R \cdot T / n^2 \cdot F^2 \cdot c \cdot A \cdot R_{\mathrm{CT}} \quad (2)$$

With ideal gas constant *R*, Faraday constant *F*, surface of the electrode *A*, temperature *T*, number of electrons *n* and concentration *c*.

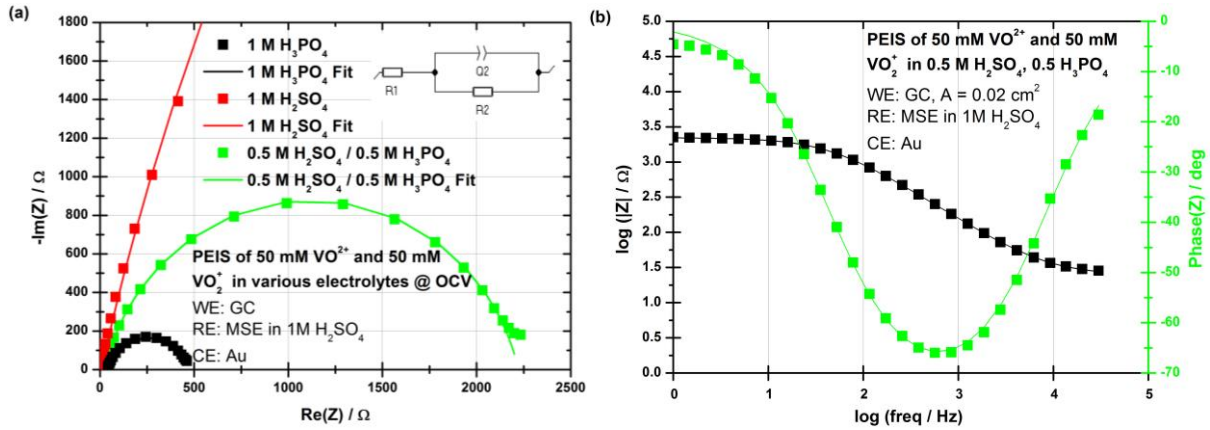

Figure 3 (a) Nyquist plot of 50 mM VO^{2+} and 50 mM VO_2^+ in various electrolytes. For clarity, only the data points recorded at high frequencies are shown for the spectrum in 1 M H_2SO_4. (b) Bode plot of 50 mM VO^{2+} and 50 mM VO_2^+ in 0.5 M H_2SO_4 / 0.5 M H_3PO_4. The recorded data points were fitted to the Randles Circuit shown as inset in Fig. 3a.

As shown in Table 2, R_{CT} is 67 times higher in the sulfuric than in the phosphoric acid system. In the mixed acid electrolyte R_{CT} is 13 higher than in phosphoric acid and 5 times lower than in sulfuric acid. The calculated capacitances are similar for all electrolytes.

	1 M H_3PO_4	**1 M H_2SO_4**	**0.5 M H_2SO_4 / 0.5 M H_3PO_4**
R_{Ohm} / Ω m²	$7.84\ 10^{-5}$	$1.21\ 10^{-5}$	$5.03\ 10^{-5}$
R_{CT} / Ω m²	$8.81\ 10^{-4}$	0.06	$4.42\ 10^{-3}$
α	0.824	0.856	0.858
Q / $Fs^{(\alpha-1)}$	$5.74\ 10^{-6}$	$3.58\ 10^{-6}$	$3.61\ 10^{-6}$
C_{DL} / F	$4.36\ 10^{-7}$	$4.32\ 10^{-7}$	$4.57\ 10^{-7}$
j_0 / A m⁻²	29.34	0.44	5.87
k_0 / cm/s	$6.09\ 10^{-4}$	$9.15\ 10^{-6}$	$1.21\ 10^{-4}$

Table 2 Fitted parameters of EIS of 50 mM VO^{2+} and 50 mM VO_2^+ in various electrolytes.

3.4 Symmetric flow cell - charge discharge tests

Charge and discharge experiments in a symmetric cell with 50 mM VO^{2+} and 50 mM VO_2^+ in 1 M sulfuric acid and 1 M phosphoric acid in both tanks were conducted with various

currents to compare the over-voltages and determine the charge transfer constant k_0. Figure 4 shows the charge/discharge curves for both systems. Due to high over-voltages, currents of 1000 and 2000 mA could not be applied on the sulfuric acid system.

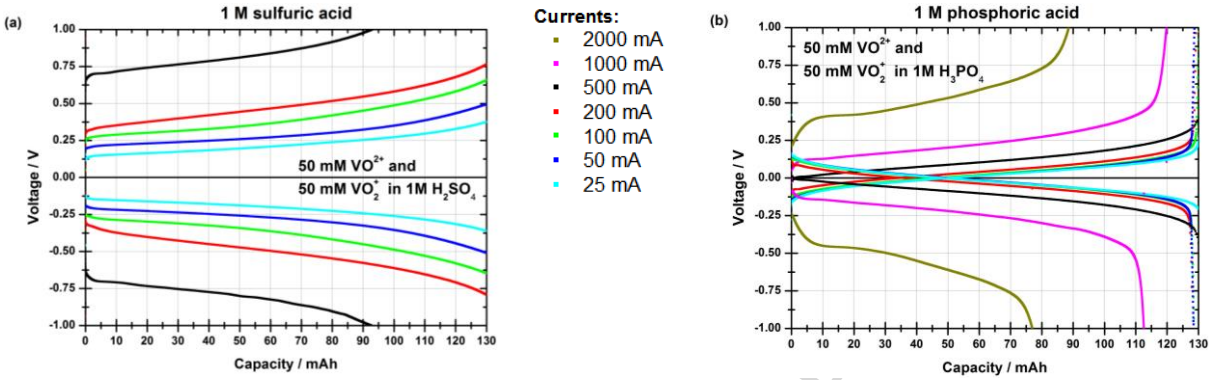

Figure 4 Charge/discharge test with SGL-GFD 4.6 electrode, Nafion N117 membrane and 60 ml 50 mM VO^{2+} and 50 mM VO_2^+ in (a) 1 M H_2SO_4 and (b) 1 M H_3PO_4.

At a state of charge (SOC) of 50%, when half of the full capacity for the respective cycle was reached, the voltage was determined for each applied current. The full capacity is determined as the capacity that is present at that point where the slope of the curve significantly changes. Figure 5 shows a pseudo Tafel plot and the exchange current density j_0 corresponds to the intersection with the ordinate.

In order to transform I_0 to k_0 the surface area has to be known. The Brunauer–Emmett–Teller (BET) surface area A^{BET} of the GFD electrodes per gram is given as 0.44 $m^2\ g^{-1}$ for untreated felts [17]. With the weight of the electrode m = (1.083 ± 0.015) g, A^{BET} = (4760 ± 66) cm^2. The value for the specific capacitance for graphite felts is a combination of the specific capacitance of the basal plane (bp) c_{DL}^{bp} = 3.2 10^{-6} F cm^{-2} and that of the edge plane (ep) c_{DL}^{ep} = 47.8 10^{-6} F cm^{-2} [18]. With heat treatment the proportion of edge planes increases [19,20]. Assuming that the electrode felts consist mostly of basal plane (94%) with a small contribution from the edge plane (6%) [18], the specific capacitance should be $c_{DL} = 0.94\, c_{DL}^{bp} + 0.06\, c_{DL}^{ep} = 5.9\ 10^{-6}\ \mathrm{F\ cm^{-2}}$. With the capacitance of the electrodes determined by EIS to be C_{DL} = 0.02055 F, the surface area of the electrode A^{DL} = 3483 cm^2. Using A^{DL} the exchange current density j_0 and thereby k_0 can be calculated from the I_0 values shown in Fig. 5. In the symmetric cell, k_0 is 38 times larger in phosphoric acid (k_0 = 9.05 10^{-5} cm s^{-1}) than in sulfuric acid (k_0 = 2.38 10^{-6} cm s^{-1}). In a full cell experiment as performed here, the R_{CT} is only part of the total resistance that leads to an over-voltage. Besides the kinetic

activation represented by R_{CT} also the membrane resistance R_{Mem}, the diffusion resistance R_{Diff} contribute to and limit k_0.

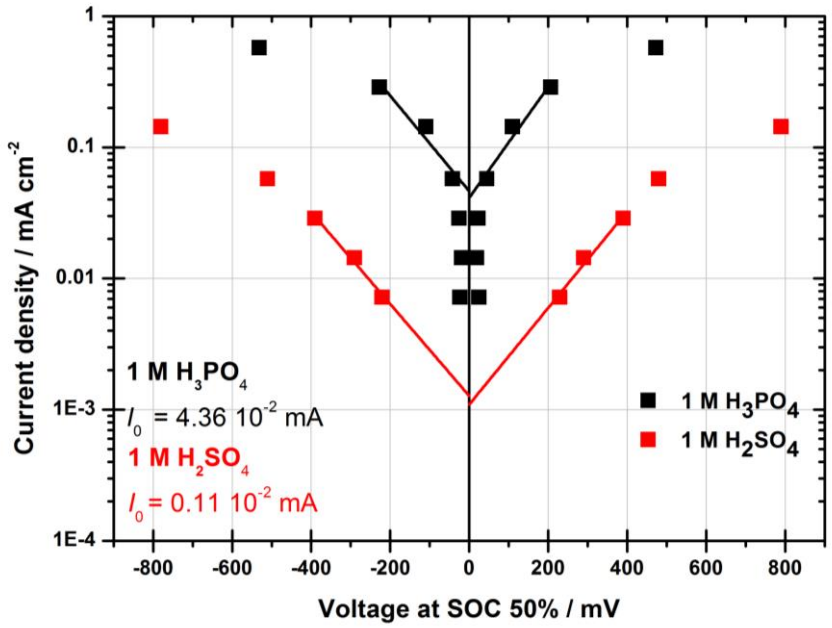

Figure 5 Pseudo Tafel plot obtained from evaluating the charge-discharge curves in Fig. 4. The current density is calculated from the currents with surface area A^{DL} from the evaluation of the double layer capacitance C_{DL}.

3.5 Chronoamperometry

Figure 6 (a) shows exemplary CA experiments ±200 mV over-potential in 1 M sulfuric acid and 1 M phosphoric acid. The inset shows as example of a potential step of 200 mV over-potential.

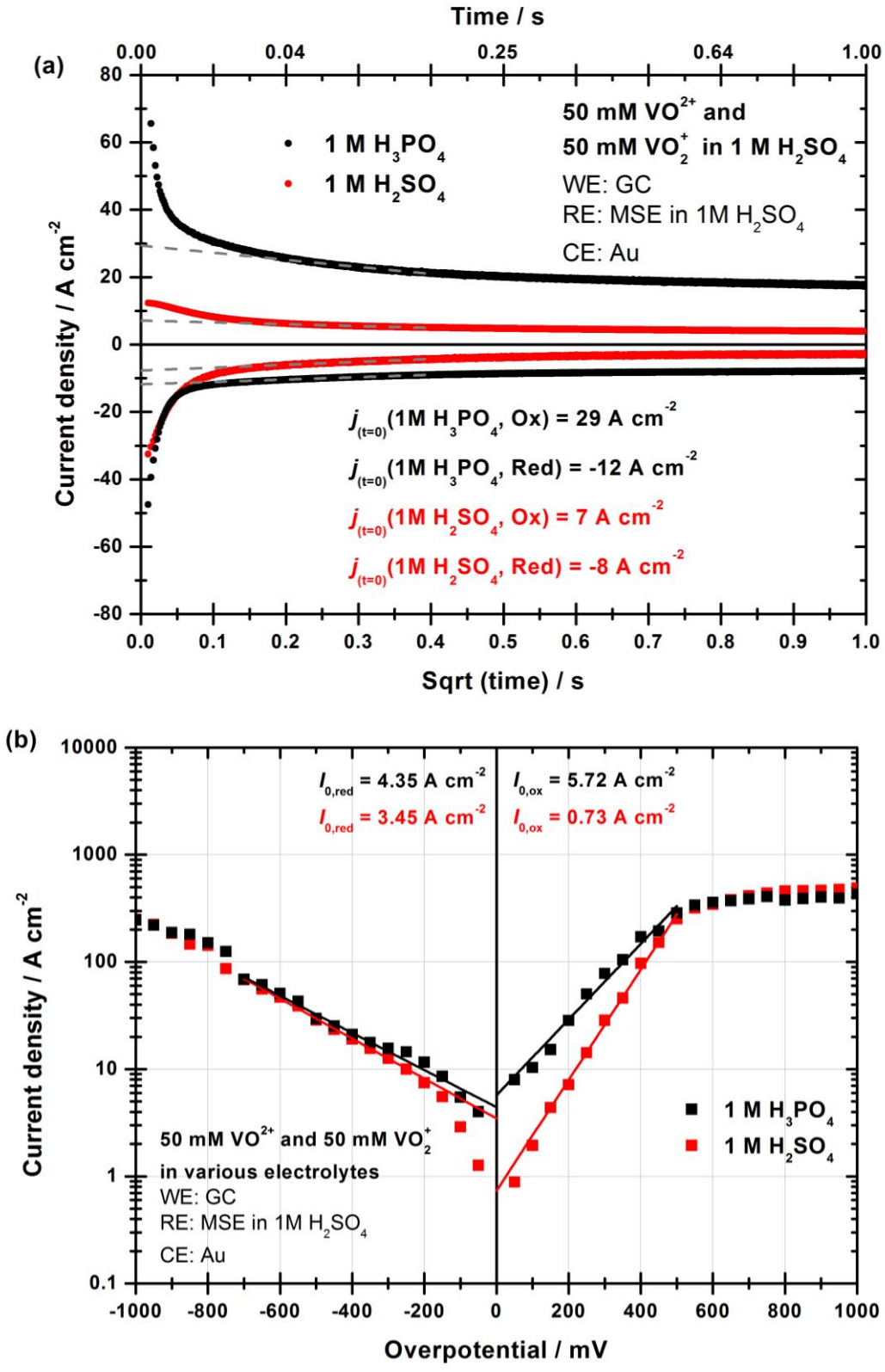

Figure 6 (a) Exemplary potentiostatic pulse experiments for 50 mM VO^{2+} and 50 mM VO_2^+ in 1 M sulfuric (red) and 1 M phosphoric acid (black). The applied potential pulse was ±200 mV and is shown for +200 mV in the inset. (b) Extrapolated faradaic current densities at $t \rightarrow 0$ s over the potential they were recorded at.

The current density response was plotted versus the square-root of time to extrapolate the faradaic current at $t \rightarrow 0$. Current densities were j ($t \rightarrow 0$) determined for all over-potentials η from ±50 to ±1000 mV and are given in Figure 6 (b). The Tafel plot shows that the cathodic area the data points for both curves are almost identical regarding position and slope. Only at small over-potentials $|\eta| < 200$ mV, the extrapolated currents are significantly higher in 1 M phosphoric acid than in 1 M sulfuric acid. Hence, for a linear fit to η = 0 the resulting apparent cathodic exchange currents $I_{0,\mathrm{red}}$ are similar. The shape of the reduction branch for both electrolytes is consistent with the investigations of Gattrell *et al.* [5] who found a very low transfer coefficient of $\alpha_{\mathrm{cathodic}} = 0.15$. In Fig. 6b the cathodic transfer coefficients are $\alpha_{\mathrm{cathodic}}^{\mathrm{H_3PO_4}} \approx \alpha_{\mathrm{cathodic}}^{\mathrm{H_2SO_4}} = 0.11$ for η >200 mV and $\alpha_{\mathrm{cathodic}}^{\mathrm{H_2SO_4}} = 0.38$ for $\eta < 200$ mV. In the anodic area both curves differ in slope and magnitude for over-potentials $\eta < 500$ mV. In that region the current values measured in 1 M phosphoric acid are significantly higher than in 1 M sulfuric acid, and the transfer coefficients are $\alpha_{\mathrm{anodic}}^{\mathrm{H_2SO_4}} = 0.31$ and $\alpha_{\mathrm{anodic}}^{\mathrm{H_3PO_4}} = 0.21$. In the region η > 500 mV both curves exhibit a plateau on which the currents are the same for both electrolyte systems. Looking at the data points before the plateau and extrapolating back to zero over-potential the apparent anodic exchange current $I_{0,\mathrm{ox}}$ in the phosphoric acid system is about 8 times higher than in the sulfuric acid system.

4. DISCUSSION

We have conducted CVs, EIS, CA and full cell tests on the VO^{2+}/VO_2^{+} redox couple in 1 M sulfuric acid, 1 M phosphoric acid and in a mixed electrolyte. All investigations indicate that electron transfer constant k_0 in the presence of PO_4^{3-} anions is higher than with SO_4^{2-} anions. A comparison of the results is shown in table 3.

	Determined from anodic branch CA	Determined from EIS at OCP	Determined from sym. flow cell
Electrolyte	k_0 / cm s^{-1}	k_0^{OCP} / cm s^{-1}	k_0^{apparent} / cm s^{-1}
1 M H_2SO_4	1.52 10^{-5}	9.15 10^{-6}	2.38 10^{-6}
1 M H_3PO_4	1.19 10^{-4}	6.09 10^{-4}	9.05 10^{-5}
0.5 M H_2SO_4 / 0.5 M H_3PO_4	----	1.21 10^{-4}	----

Table 1 Summary of all results obtained by CA, EIS and charge/discharge experiments.

However, while there is an agreement in the fact that the reaction is faster in phosphoric acid, the determined acceleration compared to sulfuric acid varies greatly. EIS was measured at OCP at small over-potentials (amplitude 10 mV). At OCP k_0^{OCP} is 67 times larger in phosphoric acid than it is in sulfuric acid. The Tafel plot obtained from CA, Fig. 6b, also shows a difference for the j ($t \rightarrow 0$) values in phosphoric acid and sulfuric acid for over-potentials -200 mV < η < 500 mV, with the largest difference around OCP. We therefore suggest that there are two over-potential dependent reaction regimes, in the anodic as well as in the cathodic branch. For over-potentials -200 mV < η < 500 mV the data points indicate the reaction is faster in phosphoric acid than in sulfuric acid, for over-potentials outside of that region, η < -200 mV and η > 500 mV, the determined current values for the two systems coincide. Gattrell *et al.* have stated that both the oxidation and the reduction of VO^{2+}/VO_2^{+} proceed via two chemical reactions (C) coupled to an electron transfer (E) [4,5]. The chemical reactions are proton transfer reactions. The set of equations proposed by Gattrell *et al*. [4,5] is presented in Fig. 7. They have found that for both oxidation and reduction three possible reaction pathways exist and that they all contribute to the current, but that their contribution varies with over-potential. For the oxidation they found that the main contributors are the sequences electron transfer E-C-C (oxidation 1, red line) and C-E-C (oxidation 2, green line) [5]. Interestingly, the modelled C-E-C reaction is characterized by a plateau for η > 150 mV. Looking at our data, we propose that in the initial over-potential region (0 mV < η < 500 mV) Oxidation 1 (E-C-C) dominates which is then replaced by Oxidation 2 (C-E-C) mechanism at η > 500 mV as major contributor. We conclude this change in reaction pathway because at η > 500 mV the current in both electrolytes exhibits a plateau as modelled for the C-E-C mechanism described in [5]. Also the fact that at η > 500 mV the measured current densities are similar, whereas before that over-potential the current density in 1 M H_3PO_4 was larger, suggests that a new rate-limiting step (with the same rate in both electrolytes) determines the rate of electron transfer. This interpretation would suggest that the rate of the E-step is faster in phosphoric acid than in sulfuric acid, therefore enabling higher currents in the former system than in the latter when the E-step is the first reaction, but that the first C-step in the CEC reaction at high over-potentials is similar in both systems and rate-limiting.

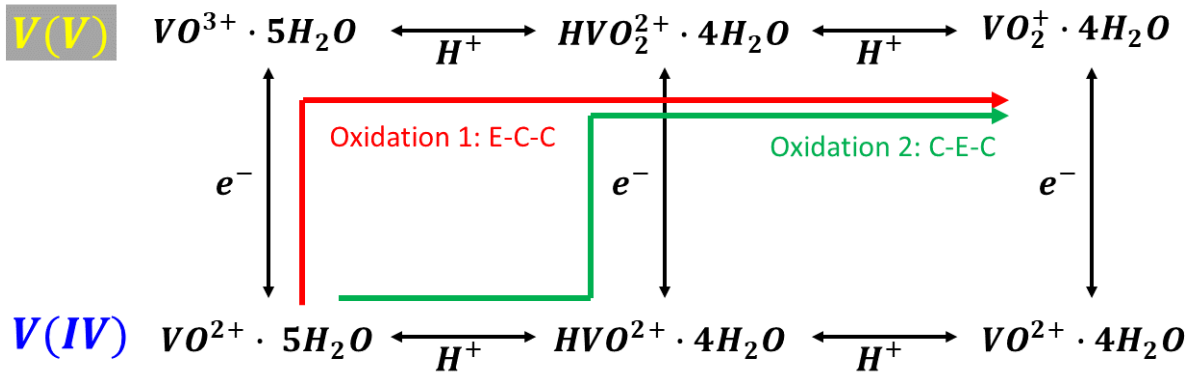

Figure 7 Possible reaction pathways for the VO^{2+}/VO_2^+ redox reaction according to [5]. Our data suggests, that for the oxidation the reaction follows Oxidation 1 (red) at low over-potentials and Oxidation 2 (green) at high over-potentials. In the latter pathway the electron transfer step (E) is preceded by a proton exchange step (C) which appears to be rate limiting.

For the reduction of VO_2^+ Gattrell *et al*. assumed that the electron transfer takes place through a layer of adsorbed intermediates at high over-potential [4]. This was hypothesized on the basis of a low apparent transfer coefficient, like the one we have observed ($\alpha_{\mathrm{cathodic}}^{\mathrm{H_3PO_4}} \approx \alpha_{\mathrm{cathodic}}^{\mathrm{H_2SO_4}} = 0.11$, see Fig. 6b). The presence of reaction intermediates was also postulated to explain EIS [6] and X-ray absorption fine structure [7] experiments. We therefore assume that the electron transfer through this layer of adsorbed species is independent of electrolyte and limits the rate at high cathodic over-potentials (η < -200 mV). As a consequence, the E-C-C reduction mechanism determines the rate only at the smallest over-potentials such 0 mV < η < -200 mV in CA.

The effects of phosphate additives on the stability of the positive electrolyte has been investigated by Ding *et al.* [21]. They showed that adding small amounts of phosphate, $c(NH_4H_2PO_4) \leq 0.2$ M, to the electrolyte (1.6 M VO_2^+ / 3 M H_2SO_4 solution at temperature of 50°C) improves the thermal stability and delays the precipitation time of VO_2^+. A charging and discharging test (1.6 M V^{3+}/VO^{2+} in 3.0 M H_2SO_4) has been conducted and has shown improved performance regarding long-term stability and energy efficiency (83%, 300 cycles) with 0.2 M $NH_4H_2PO_4$ additive [21]. The results also indicate that the introduction of phosphate reduces the over-potential within the cell, however, no quantitative values were obtained. Earlier heating/cooling studies from Zhang *et al.* showed that adding 3 wt% Na_3PO_4 notably improves the thermal stability (-5 to 40°C) of 2 M V(III), V(IV) and V(V) in 5 M sulphate solution [22]. The time without precipitation at aforementioned temperature range has been extended in case of all three investigated vanadium species by many days. In our

experiments, we have observed that after a few days a precipitation occurs in the phosphoric acid solution which is re-dissolvable by heating to 70°C for 30 min.

5. CONCLUSION

As other researchers before, we conclude that the VO^{2+}/VO_2^+ redox reaction is an intricate combination of electron transfer and chemical reactions [4–7]. Our previous experiments have clearly shown that the reaction is not catalysed by oxygen functional groups on the surface of carbon electrodes [3,6,8] which is in agreement with other research groups [23–27]. In this publication we are able to show that the electron transfer reaction part of the VO^{2+}/VO_2^+ redox reaction can be considerably accelerated when 1 M phosphoric acid is used as supporting electrolyte instead of 1 M sulfuric acid. However, we have also shown that the change in supporting electrolyte only accelerates the electron transfer part of the reaction. The coupled chemical reactions that limit the rate at high anodic over-potentials, or the electron transfer through a layer of reaction intermediates at cathodic over-potentials which seems to slow down the reaction, is independent of the employed anion. Nevertheless, in a laboratory scale flow cell that employed dilute vanadium electrolyte (100 mM vanadium), we were able to show that the over-voltages can be significantly lower in phosphoric acid than compared to sulfuric acid. Considering that commercial VRFB electrolyte contains phosphoric acid as a stabilising agent, it can be worthwhile to explore the ideal ratio of H_2SO_4/H_3PO_4 in terms of kinetics and stability for technical and commercial systems.

6. REFERENCES

[1] C. Ponce de León, A. Frías-Ferrer, J. González-García, D. A. Szánto, F. C. Walsh, J. Power Sources 160 (2006) 716–732.

[2] A.Z. Weber, M.M. Mench, J.P. Meyers, P.N. Ross, J.T. Gostick, Q. Liu, J. Appl. Electrochem. 41 (2011) 1137–1164.

[3] J. Friedl, U. Stimming, Electrochim. Acta 227 (2017) 235–245.

[4] M. Gattrell, J. Qian, C. Stewart, P. Graham, B. MacDougall, Electrochim. Acta 51 (2005) 395–407.

[5] M. Gattrell, J. Park, B. MacDougall, J. Apte, S. McCarthy, C.W. Wu, J. Electrochem. Soc. 151 (2004) A123.

[6] H. Fink, J. Friedl, U. Stimming, J. Phys. Chem. C 120 (2016) 15893–15901.

[7] J. Maruyama, T. Shinagawa, A. Hayashida, Y. Matsuo, H. Nishihara, T. Kyotani, ChemElectroChem 3 (2016) 650–657.

[8] J. Friedl, C.M. Bauer, A. Rinaldi, U. Stimming, Carbon N. Y. 63 (2013) 228–239.

[9] I. Derr, A. Fetyan, K. Schutjajew, C. Roth, Electrochim. Acta 224 (2017) 9–16.

[10] G.A. Webb, Annual Reports on NMR Spectroscopy Band 62, Academic Press Inc., 2007.

[11] S.E. O'Donnell, M.T. Pope, J. Chem. Soc. Dalt. Trans. (1976) 2290.

[12] M.J. Gresser, A.S. Tracey, K.M. Parkinson, (1986) 6229–6234.

[13] M.P. Williamson, Prog. Nucl. Magn. Reson. Spectrosc. 73 (2013) 1–16.

[14] International Union of pure and applied Chemistry, Standard Potentials in Aqueous Solution., CRC Press, New York, 1985.

[15] A. Bard, L. Faulkner, Electrochemical Methods: Fundamentals and Applications, Second, John Wiley and Sons, New York, 2001.

[16] B. Hirschorn, M.E. Orazem, B. Tribollet, V. Vivier, I. Frateur, M. Musiani, Electrochim. Acta 55 (2010) 6218–6227.

[17] R. Schweiss, T. Oelsner, F. Dörfler, A. Davydov, S. Wöhner, in:, Int. Flow Batter. Forum 2011, 2011, pp. 44–45.

[18] T.J. Rabbow, A.H. Whitehead, Carbon N. Y. 111 (2017) 782–788.

[19] T.J. Rabbow, M. Trampert, P. Pokorny, P. Binder, A.H. Whitehead, Electrochim. Acta 173 (2015) 17–23.

[20] T.J. Rabbow, M. Trampert, P. Pokorny, P. Binder, A.H. Whitehead, Electrochim. Acta 173 (2015) 17–23.

[21] C. Ding, X. Ni, X. Li, X. Xi, X. Han, X. Bao, H. Zhang, Electrochim. Acta 164 (2015) 307–314.

[22] J. Zhang, L. Li, Z. Nie, B. Chen, M. Vijayakumar, S. Kim, W. Wang, B. Schwenzer, J. Liu, Z. Yang, J. Appl. Electrochem. 41 (2011) 1215–1221.

[23] M.A. Miller, A. Bourke, N. Quill, J.S. Wainright, R.P. Lynch, D.N. Buckley, R.F. Savinell, J. Electrochem. Soc. 163 (2016) A2095–A2102.

[24] A. Bourke, R.P. Lynch, D.N. Buckley, ECS Trans. 53 (2013) 59–67.

[25] A. Bourke, N. Quill, R.P. Lynch, D.N. Buckley, ECS Trans. 61 (2014) 15–26.

[26] R. Schweiss, C. Meiser, F. Wei, T. Goh, ChemElectroChem (2017) 1–7.

[27] J. Langner, M. Bruns, D. Dixon, A. Nefedov, C. Wöll, F. Scheiba, H. Ehrenberg, C. Roth, J. Melke, J. Power Sources 321 (2016) 210–218.